International Journal of Information, Control and Computer Sciences
ISSN: 2517-9942
Vol:2, No:8, 2008

Deficiencies of Lung Segmentation Techniques using CT Scan Images for CAD

Nisar Ahmed Memon, Anwar Majid Mirza, and S.A.M. Gilani

***Abstract*—**Segmentation is an important step in medical image analysis and classification for radiological evaluation or computer aided diagnosis. This paper presents the problem of inaccurate lung segmentation as observed in algorithms presented by researchers working in the area of medical image analysis. The different lung segmentation techniques have been tested using the dataset of 19 patients consisting of a total of 917 images. We obtained datasets of 11 patients from Ackron University, USA and of 8 patients from AGA Khan Medical University, Pakistan. After testing the algorithms against datasets, the deficiencies of each algorithm have been highlighted.

***Keywords*—**Computer Aided Diagnosis (CAD), Mathematical Morphology, Medical Image Analysis, Region Growing, Segmentation, Thresholding,

I. Introduction

HIGH-resolution X-Ray computed tomography (CT) is the standard for pulmonary imaging. Depending on the scanner hardware, CT can provide high spatial and high temporal resolution, excellent contrast resolution for the pulmonary structures and surrounding anatomy, and the ability to gather a complete three-dimensional (3-D) volume of the human thorax in a single breath hold [1]. Pulmonary CT images have been used for applications such as lung parenchyma density analysis [2],[3], airways analysis and nodule detection for diagnosing early lung cancer. A precursor to all of these quantitative analysis applications is lung segmentation. Several authors [4],[5] have presented the variety of schemes which use automatic and semi-automatic methods for extraction of lungs from CT scan images. These image segmentation algorithms give promising results.

However there are several issues related to image segmentation that require detailed review. One of the common problems encountered in image segmentation is choosing a suitable approach for isolating different objects from the background. For example in case of Lung CT, segmentation can be performed by making use of excellent contrast between air and surrounding tissues. However, this approach fails when lung is affected by high density pathology. Moreover, for computer analysis such as detection and quantification of abnormal areas, it is vital that the entire and perfectly complete lung part of the image is provided and no part, as present in the original image, be eradicated [6]. An additional problem is the inaccurate lung segmentation due to the juxtapleural nodules present at the border of chest wall in lung parenchyma. Different groups of authors have used the technique of rolling ball algorithm in order to overcome the loss of juxtapleural nodules. This approach again has the problem of the fix size of the structuring element used for morphological operations (e.g. dilation , erosion , opening and closing) for filling the gaps or smoothing the contours of the segmented lungs. In this paper, we have highlighted these limitations by implementing the different algorithms and then have analyzed the results.

Manuscript received on July 10, 2006. This work was supported in part by the Quaid-e-Awam University, Pakistan under faculty development programme.

N. A Memon is graduate student of Faculty of Computer Science and Engineering at GIK Institute, Pakistan (e-mail: memon_nisar@yahoo.com).
A. M. Mirza is with the Ghulam Ishaq Khan Institute of Engineering Sciences and Technology, NWFP, Paksitan (e-mail: mirza@giki.edu.pk).
S. A. M. Gilani is with Ghulam Ishaq Khan Institute of Engineering Sciences and Technology, NWFP, Paksitan (e-mail: asif@giki.edu.pk).

II. Background

This section describes the different lung segmentation techniques reported by different authors. Riccardo et al. [7] has provide the novel segmentation technique that combines a knowledge-based segmentation system with a sophisticated active contour model. This approach exploits the guidance of a higher-level process to robustly perform the segmentation of various anatomic structures to be segmented is defined statistically in terms of probability density functions of parameters such as location, size, and image intensity (e.g computed tomographic (CT) attenuation value). Preliminary results suggest that the performance of the algorithm at chest and abdominal CT is comparable to that of more traditional segmentation techniques like region growing and morphologic operators. In some cases, the active contour-based techniques may outperform standard segmentation methods due to its capacity to fully enforce the available a priori knowledge concerning the anatomic structure of interest. The active contour algorithm is particularly suitable for integration with high level image understanding frameworks, providing robust and easily controlled low-level segmentation tool. Binsheng et al. [8] has used the method of selecting the threshold by analyzing the histogram. The threshold is then used to initially separate the lung parenchyma from the other anatomical structures on the CT images. As the apparent density of voxels and bronchial walls in the lungs differ, structures with higher densities including some higher density nodules could be grouped into soft tissues and bones, leading to an incomplete extraction of lung mask. To obtain complete hollow free lung mask, morphological closing is applied. Spherical shape of the structural element is chosen for morphological operator and the filter size is approximately determined. With the help of 3D mask, the lungs can be readily extracted from the original chest CT images. Shiying et al. [5] have presented a fully automatic method for identifying lungs in 3D pulmonary X-Ray CT images. The method is divided into three main steps: 1) lung region is extracted from CT-Scan image by gray-level thresholding. 2) left and right lungs are separated by identifying the anterior and posterior junctions by dynamic programming. 3) sequence of morphological operations is used to smooth the irregular boundary along the mediastinum in order to obtain results consistent with those obtained by manual analysis, in which only most central pulmonary arteries are excluded from the lung region. Samuel et al. [9] has introduced the use of Ball-Algorithm for the segmentation of lungs. At first stage, each CT-Image is gray level thresholded to segment the thorax from background and then the lungs from the thorax. In next step, rolling ball algorithm is applied to the lung segmentation contours to avoid the loss of juxtapleural nodules. The authors have used 17-case database for verifying the results with the help of radiologists.

III. Implementation

We have implemented three algorithms. The algorithms are: (1) the thresholding and region growing algorithm proposed by Shiying Hu et al. [5], Ayman Al-Baz, et al. [10] and Ayman Al-Baz et al. [11] (2) the thresholding and morphology algorithm proposed by Binsheg Zhao et al. [8], and (3) the thresholding and rolling ball algorithm proposed by Samuel G. Armato III et al. [9]. We term these algorithms as Scheme-I, Scheme-II and Scheme-III respectively.

A. Scheme-I (Thresholding + Region Growing)

The authors have selected an optimal thresholding scheme which selects the threshold based on the object and background pixel means. Once the threshold has been selected and applied, region growing and connectivity analysis are used to extract the exact cavity region with accuracy. The scheme is discussed as under:

(a) Optimal Thresholding : Across a population of subjects and sample images, usually small variations in tissue density are exhibited. Optimal thresholding is an automatic selection method that allows to accommodate the small density variations in tissues. We assume for each image that the image can be separated into two types of voxels, as characterized by the density differences between the two anatomical structures (usually these density-based characterizations can be directly obtained from CT scan equipment): 1) voxels within the very dense body and chest wall structures (the *body* voxels), and 2) low-density voxels in the lungs or in the air surrounding the body of the subject (the *nonbody* voxels). Thus, the essential aim of optimal thresholding is to separate the body voxels (soft lung tissue) from the lung cavities (non-body voxels). The lung cavities are usually low-density structures. Since low density structures are usually represented as relatively dark regions on CT scans, contrast-based segmentation is possible.

(b) Iterative Thresholding: The segmentation threshold selection is best described as an iterative procedure. Let T^i be the segmentation threshold after the i^{th} step. To choose a new segmentation threshold, we apply T^i to the image to separate the voxels into body and nonbody voxels. Let μ_0 and μ_n be the mean then new threshold will be:

$$T^{i+1} = \frac{1}{2}(\mu_b + \mu_n) \qquad (1)$$

This iterative approach continues until the threshold converges. In order to start the iteration, the mean value of the pixels is selected as the initial threshold T^0 for the computation of the threshold iteratively. The flow chart of the iterative algorithm is shown in Fig.1.

(c) Connectivity Analaysis: After applying the optimal threshold, the nonbody voxels (white in the pictures) will correspond to the air surrounding the body, the lungs, and other low-density regions within the image volume (i.e., gas in the bowel). Our next step is the connectivity analysis of the thresholded image and the segmentation of the lung cavities from the thresholded image via region growing.

(d) Selection of Seed Pixel: Essentially, a seed pixel must be selected from which the region growing may commence. Since the aim of this part of the segmentation process is the removal of the dark areas adjoining the lung parenchyma, a seed pixel must be selected from the dark region. The approach selected here finds the minimum pixel from the image on the boundary. This is a dark pixel (grey level 0) in most cases.

(e) Region growing: Once the dark pixel coordinates are selected (background air), region growing commences in the form of marking all the pixels which lie in the 8-connected neighbourhood of the seed pixel. The process is repeated for each pixel until all the black pixels are marked in the image which adjoin the areas of the lung parenchyma. This essentially deletes the dark regions that are connected to the border of the image. To distinguish between the white regions already present in the lung parenchyma and the white regions

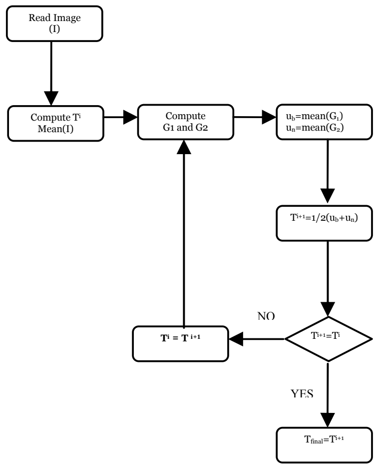

Fig. 1 Flow Chart of iterative Algorithm

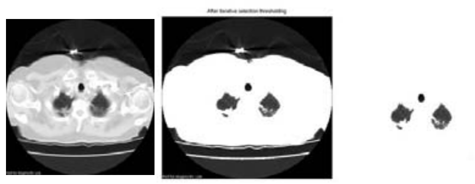

(Threshold = 119)

(a) – Original, thresholded and segmented image of the beginning of the lung

(Threshold = 121)

(b) – Original, thresholded and segmented image of the middle of the lung

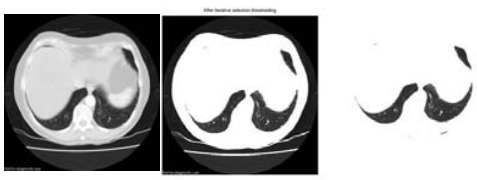

(Threshold = 118)

(c) – Original, thresholded and segmented image

Fig. 2 Original and segmented images with thresholds on which thresholding was performed

generated because of the background air volume, the white regions of the lung parenchyma are tagged before region growing commences. This is because if the region-growing algorithm was only moderated according to gray-levels, the region growing algorithm would extend on the complete image. The enclosing property of the white parenchyma is retained by tagging the white parenchyma before region growing commences from the border regions towards the inside.

The Fig. 2 shows the results of thresholding and region growing for the different images taken from the different part of lung parenchyma like initial, middle and end parts of the lung.

B. Scheme-II (Thresholding + Morphology)

In Scheme-II, Binsheg Zhao et al. [9] have used optimal threshold after analyzing the histogram of the chest CT Scan image for segmenting the thorax area from each CT Scan image. The morphological closing is then applied to resultant images. The overall flow chart of the scheme is shown in Fig. 3. In order to make the threshold selection method automatic for implementation purpose, we have used the iterative method discussed in part A of section III. Once the threshold is calculated it is applied to each CT-Scan image which gives the binary image as the result. The voxels having a density lower than the threshold value are recognized as lung candidates and assigned value 1 and appear white, whereas other voxels are assigned the value of 0 and appear black as shown in Fig. 4(b).

Due to their low densities, both lung parenchyma and background will be classified as the "Lung" on the resultant binary images. As the lung parenchyma is usually completely isolated from the background by the chest-wall, it can be readily determined by labeling 3D connected components (i.e grouping geometrically connected voxels that have value 1 and assigning an identical number to the voxels in each individual group) and selecting the largest component that does not touch any margin of the images. The resultant image is shown in Fig. 4(c). As the apparent density of the vessels and bronchial walls in the lung differ, structures with higher densities including some higher density nodules could be grouped into soft tissues and bones, leading to an incomplete extraction of lung mask as shown in Fig. 4(c). To obtain a complete, hollow-free lung mask, morphological closing is applied. Fig. 4(d) shows the result. Spherical shape of structural element is chosen for the morphological operator. We chose the ball of radius 10 pixels for the closing operation. The final lung parenchyma has been extracted with the help of lung mask. The final result is shown in Fig. 4(e). After implementing the algorithm of scheme-II, we applied this scheme on the images received from AGA Khan University Hospital, Pakistan. The results are shown in Fig. 5.

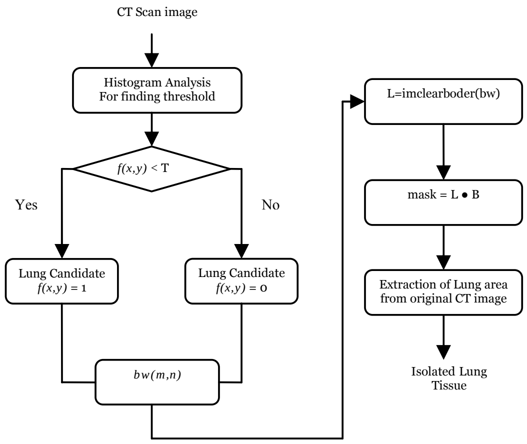

Fig. 3 Flow Chart of Scheme-II

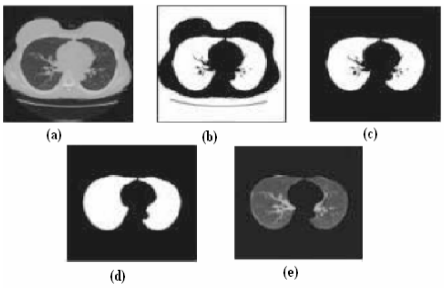

Fig. 4 (a) Original image (b) Binary image (c) Isolated lungs (d) Hollow-free lung mask (e) Lung Parenchyma extracted from (a) using (c)

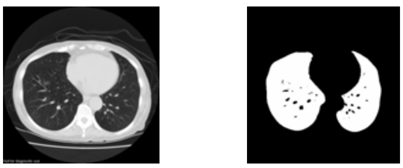

(a) original image (b) Thresholded image

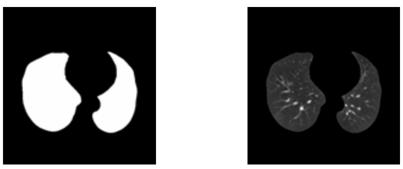

(c) hollow free lung mask (d) extracted lung parenchyma

Fig. 5 Results of Scheme-II
Source: AGA Khan University Hospital database
Patient : Anonymous 19863 (Slice No. 19)

C. Scheme-III (Thresholding + Ball Algorithm)

Samuel G. Armato III et al. [8] have used the gray level thresholding methods for each CT-Scan to segment the thorax from background and then lungs from the thorax. A rolling ball algorithm is then applied to the lung segmentation contours to avoid the loss of juxtapleural nodules. The flow chart of the algorithm is shown in Fig. 6. In order to implement algorithm, we first used the method of gray-level thresholding. After computation of threshold it was applied to the corresponding CT-Scan image. The original CT Scan image is shown in Fig. 7(a). After thesholding we have a binary image. The voxels having a density lower than the threshold value are recognized as lung candidates and assigned the value 1, whereas other voxels are assigned the value of 0 as shown in Fig. 7(b). As the lung parenchyma is usually completely isolated from the background by the chest wall, it is readily determined by labeling 3D-connected components and selecting the largest component that does not touch any margin of the image. The result is shown in Fig. 7(c). The gaps in the lung parenchyma due to other anatomical structures, there are some holes which are filled in order to get the hollow free lung mask as shown in Fig.7(d). Due to nodules present at lung-wall the parts of lungs have been eradicated and indentations are produced as shown in Fig. 7(e). So in order to overcome this loss of juxtapleural nodules rolling ball algorithm is applied to fill the indentations. Spherical shape of structuring element of radius 10 pixels has been used. Fig. 7(f) shows the result. Again holes are filled to get the complete lung mask as shown in Fig. 7(g). Finally the lung parenchyma has been extracted from the original CT Scan image with help of mask. The Fig. 7(h) depicts the result. After implementing the algorithm of scheme-III, we used it to test on the image database received us from Ackron University, USA. The results are shown in Fig. 8. The results show that the algorithm gives the promising results. It fills the indentations produced by the juxtapleural nodules.

IV. RESULTS

After implementing the above schemes we found limitations from each scheme and are described below:

A. Limitations of Scheme-I

After applying Scheme-I on the images shown in Fig. 2, we applied this algorithm on the images received from AGA Khan University Hospital, Pakistan and Ackron University, USA. Fig. 9 shows the slice from the image database received from Ackron University, USA and its thresholded image which give the promising results. However, the results shown in Fig. 10 depict that the algorithm does not give the satisfied results. Fig. 10(b) shows that half of the image has been washed out. This is

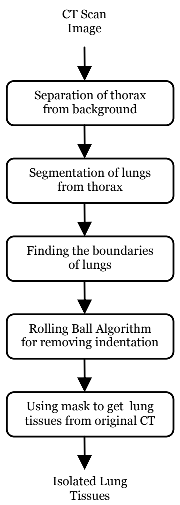

Fig. 6 Flow Chart of Scheme-III

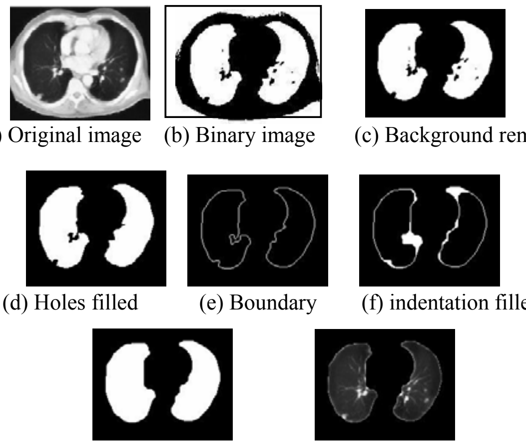

(a) Original image (b) Binary image (c) Background removed

(d) Holes filled (e) Boundary (f) indentation filled

(g) Hollow free lung mask (h) extracted lung parenchyma

Fig. 7 Process Cycle of Scheme-III

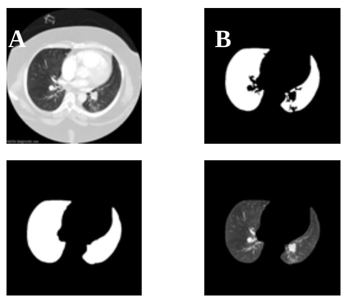

Fig. 8 Results of Scheme-III
(a) Original image (b) Thresholded image (c) Hollow free lung mask (d) Extracted Lungs
Source: Ackron University database
Patient : TestPatient 8, Jane-4 (Slice No. 43)

again because of same intensity values of lung tissues available in lung parenchyma. Thus it can easily be concluded that the Scheme-I does not work for the images when there is overlapping of intensities in lung parenchyma and surrounding chest wall. This is very serious shortcoming of the Scheme-I which may lead to inaccurate diagnosis of disease.

B. Limitations of Scheme- II

While testing the database slice by slice it was found that the spherical structuring element selected for morphological opening to get the hollow-free lung mask was almost working for the entire database of the patient. However for few slices it did not give promising results. The results are shown in Fig. 11. Thus it was observed that ball size selected for morphological closing did not work for the entire database of all single patient. Some times a ball of specified size worked for one patient while it was not sufficient for another patient. Thus we have to vary the ball size patient by patient which makes the algorithm semi-automatic. Hence it can be concluded that the main limitation of scheme-II is the size of the ball selected for morphological operation.

C. Limitations of Scheme-III

While testing the database of each patient slice by slice, we observed that ball algorithm was almost working for each patient's database, but for few slices it did not give satisfied results. As shown in Fig. 12 and Fig. 13. Also applying the rolling ball algorithm for overcoming the loss of juxtapleural nodules is an additional processing time overhead. From Fig. 12, we can see that the rolling ball algorithm however fills the indentations of left side of the lung but does not completely fill the indentations produced in the right side of the lung. Also from Fig. 13, we can observe that the ball algorithm includes the unnecessary areas as the lung region, (not actually the part of the lung). Thus from experiments we can conclude that the scheme-III has the following very serious short comings: (i) Fixed ball size (ii) Processing time overhead (iii) Inclusion of unnecessary areas as lung regions.

V. DISCUSSION

In this work, we have studied the performance of the different segmentation techniques that are used in Computer Aided Diagnosis (CAD) systems using thorax CT Scans. These methods for segmentation give good results on test databases of reasonable size. There is still much room to work on Computer Aided Diagnosis in CT imaging. CT lung density is influenced by the factors such as subject tissue volume, air volume, image acquisition protocol, physical material properties of lung parenchyma and transpulmonary pressure. These factors make the selection of gray-level segmentation threshold difficult, as different thresholds are

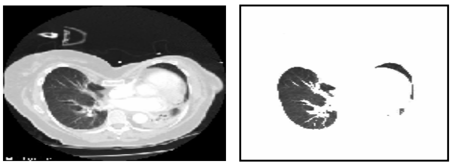

(a) Original image (b) Segmented image

Fig. 9 Results of Scheme-I

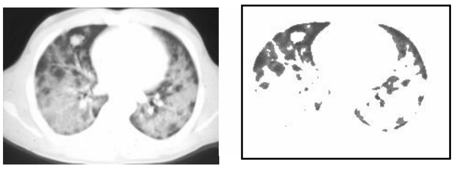

(a) original image (b) segmented image

Fig. 10 Results of Scheme-I with deficiencies

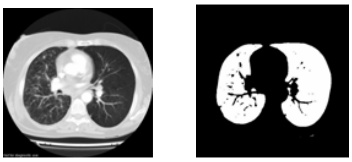

(a) original image (b) thresholded image

(c) Lung mask (d) extracted lung

Fig. 11 Results of Scheme-II with deficiencies
Source: AKU University database
Patient : Anonymous 19863 (Slice No.27)

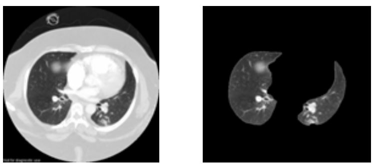

(a) Original image (b) Segmented image
Fig. 12 Results of Scheme-III with deficiencies

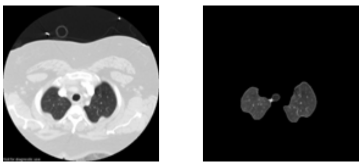

(a) Original image (b) Segmented image
Fig. 13 Results of Scheme-III with deficiencies

likely required for different subjects. The selection of optimal threshold by iterative method is one possible solution. But again due to different density of anatomical structures on each slide as discussed above, there is need of computing the threshold for each slide which is costly from computational point of view. Thus there is a need of sophisticated algorithm which can calculate a single threshold for entire database of a single patient. Also, the algorithms reported so far have used the databases of slice thickness usually varying in (5-10 mm). But with the advent of modern MSCT scanners and their possibility to acquire submillimeter slice data over the whole thorax with a single breath-hold, software algorithms for CAD for the diagnosis of lung cancer must be improved using these databases having slice thickness of 1 mm or less.

References

[1] Hoffman, E. A, and McLennan, G., "Assessment of the pulmonary structure-function relationship and clinical outcomes measures: Quantitative volumetric CT of the lung", Academic Radiology, vol. 4, no. 11, pp. 758-776, 1997.

[2] Hedlund, L.W., Anderson, R.F., Goulding, P.L., Beck, J. W., Effmann, E.L.and Putman, C.E, "Two methods for isolating the lung area of a CT scan for density information", Radiology, vol. 144, pp. 353-357, 1982.

[3] Uppaluri, R., Mitsa, T., Sonka, M., Hoffman, E. A., and Mclemman, G., "Quatification of pulmonary emphysema from lung CT images using texture analysis", Amer. J. Resp. Crit. Care Med. vol. 156, no. 1 pp. 248-254, 1997.

[4] Julian Kerr, "The TRACE method for Segmentation of Lungs from Chest CT images by Deterministic Edge Linking", University of New South Wales, Department of Artificial Intelligence, Australia, May 2000.

[5] Shiying Hu, Eric A.Huffman, and Joseph M. Reinhardt, "Automatic Lung Segementation for Accurate Quantitiation of Volumetric X-Ray CT images", IEEE Transactions on Medical Imaging, vol. 20, No. 6, June 2001.

[6] Manzoor Ahmed Khawaja, Muhammed Zaheer Aziz, Nadeem Iqbal, "Effectual Lung Segmentation for CAD System Using CT Scan Images",IEEE Transactions, INMIC, National Univeristy of Emerging Sciences, FAST Lahore, Pakistan, 2004.

[7] Riccardo Boscolo, Mathew S. Brown, Michael F. McNitt-Gray, "Medical Image Segmentation with Knowledge-guided Robust Active Contours", Radiographics, vol. 22, pp. 437-448, 2002.

[8] Binsheng Zhao, Gordon Gamsu, Michelle S. Ginsberg, "Automatic detection of small lung nodules on CT utilizing a local density maximum algorithm", Journal of Applied Clinical Medical Physics, vol. 4, No. 3, summer 2003.

[9] Samuel G. Armato III, Maryellen L. Giger and Catherine J. Moran, "Computerized Detection of Pulmonary Nodules on CT Scans", RadioGraphics, vol. 19, pp. 1303-1311, 1999.

[10] Ayman El-Baz, Aly A. Farag, Robert Falk, Renato La Rocca, "Detection, Visualization and identification of Lung Abnormalities in Chest Spiral CT Scan: Phase-I", International Conference on Biomedical Engineering, Cairo, Egypt, 12-01-2002.

[11] Ayman El-Baz, Aly A. Farag, Robert Falk, Renato La Rocca, "A Unified Approach for Detection, Visualization and Identification of Lung Abnormalities in Chest Spiral CT Scan", Proceedings of Computer Assisted Radiology and Surgery, London 2003.